Effects of band broadening and shape of the density of states on the magnetic phase diagram

2006 J. Phys.: Condens. Matter 18 7227

(http://iopscience.iop.org/0953-8984/18/31/017)

INSTITUTE OF PHYSICS PUBLISHING JOURNAL OF PHYSICS: CONDENSED MATTER

J. Phys.: Condens. Matter **18** (2006) 7227–7236 doi:10.1088/0953-8984/18/31/017

Effects of band broadening and shape of the density of states on the magnetic phase diagram

Kyoo Kim, Unjong Yu, Beom Hyun Kim and B I Min

Department of Physics, Pohang University of Science and Technology, Pohang 790-784, Korea

Received 29 May 2006
Published 21 July 2006
Online at stacks.iop.org/JPhysCM/18/7227

Abstract

We have revisited metallic ferromagnetism to examine the effects of band broadening due to electron–electron interaction on the magnetic phase diagram. Based on the generalized single band tight-binding Hamiltonian, we have explored the condition when the magnetization jumps discontinuously, by comparing results obtained by the local minima search and the total energy minimization. We have also investigated how the shape of the density of states (DOS) affects the magnetic phase diagram. We have found that a system with the DOS shape of a concave-type could have the discontinuous magnetization jump as the effective Stoner parameter increases.

Hirsch [1–4] has reported a new mechanism for metallic ferromagnetism based on the generalized single band tight-binding (TB) Hamiltonian. He has studied the effects of the higher-order interaction terms beyond the Hubbard on-site Coulomb interaction, such as the inter-site Coulomb interaction, the exchange interaction, and the pair-hopping interaction, on the magnetic properties. Higher-order terms dress electrons and eventually change the bandwidth. In this way, he took into account the band broadening effect in addition to the normal Stoner exchange band-splitting effect, and found that the ferromagnetism is enhanced by the band broadening effect.

In obtaining the magnetic phase diagram, Hirsch has employed the method of local minima search and used the simple model density of states (DOS): the square-type DOS and the TB-DOS of a one-dimensional lattice chain (1D TB-DOS). Barreteau *et al* [5] also analysed the condition for metallic ferromagnetism in the framework of the TB approximation and examined the effects due to the renormalization of the hopping integrals by the inter-site Coulomb interaction. They found that the effects are strongly dependent on the shape of the DOS as well as on the relative values of the inter-site Coulomb interaction. They pointed out that, to obtain the correct magnetization, one should minimize the total energy with respect to the magnetization, instead of finding just local minima as Hirsch did.

In this study, we have studied systematically the issues addressed by Hirsch and Barreteau *et al* in metallic ferromagnetism. We have investigated how the shape of the DOS affects the magnetic phase diagram and when the total energy minimization and the local minima search

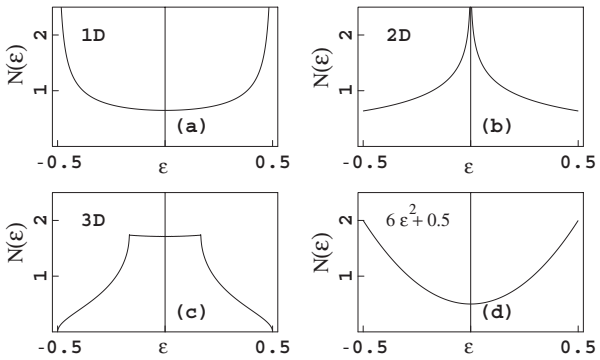

Figure 1. (a) TB-DOS of one-dimensional lattice chain (1D TB-DOS), (b) TB-DOS of the 2D square lattice (2D TB-DOS), (c) TB-DOS of the 3D simple-cubic lattice (3D TB-DOS), (d) the parabolic DOS ($N(\varepsilon) = 6\varepsilon^2 + 0.5$).

yield different results for the equilibrium magnetization. For this purpose, we have considered several types of DOS, such as the 1D TB-DOS, TB-DOSs of the 2D square lattice (2D TB-DOS) and the 3D simple-cubic lattice (3D TB-DOS), and the parabolic DOS, as well as the square-type DOS, as shown in figure 1. We have found that the total energy minimization is essential to find the correct magnetic phase diagram and that the magnetic phase diagram is sensitive to the shape of the DOS profile.

The following is a generalized single band TB Hamiltonian considered by Hirsch [1],

$$H = -t \sum_{\langle ij\rangle\sigma} \left(c^{\dagger}_{i\sigma} c_{j\sigma} + \text{H.c.} \right) + U \sum_{i} n_{i\uparrow} n_{i\downarrow} + V \sum_{\langle ij\rangle} n_i n_j + J_{\text{ex}} \sum_{\langle ij\rangle\sigma\sigma'} c^{\dagger}_{i\sigma} c^{\dagger}_{j\sigma'} c_{i\sigma'} c_{j\sigma} + J_{\text{ph}} \sum_{\langle ij\rangle} \left(c^{\dagger}_{i\uparrow} c^{\dagger}_{i\downarrow} c_{j\downarrow} c_{j\uparrow} + \text{H.c.} \right). \tag{1}$$

Here U, V, J_{ex}, and J_{ph} are the Hubbard on-site Coulomb interaction, the inter-site Coulomb interaction, the exchange interaction, and the pair-hopping, respectively.

From equation (1), one gets the mean-field Hamiltonian,

$$\begin{aligned} \overline{H} &= \sum_{k\sigma} \alpha_\sigma \varepsilon^0_k c^{\dagger}_{k\sigma} c_{k\sigma} + \sum_{k\sigma} \tilde{u} D n_{-\sigma} c^{\dagger}_{k\sigma} c_{k\sigma} \\ &\Rightarrow \sum_{k\sigma} \left(\alpha_\sigma \varepsilon^0_k - \frac{\sigma}{2} \tilde{u} D m \right) c^{\dagger}_{k\sigma} c_{k\sigma}, \qquad \text{within constant} \\ &\equiv \sum_{k\sigma} \varepsilon_{k\sigma} c^{\dagger}_{k\sigma} c_{k\sigma}, \end{aligned} \tag{2}$$

where ε^0_k, $\varepsilon_{k\sigma}$, and m are the bare electron energy, the quasi-particle energy, and the magnetization, respectively. α_σ represents the spin-dependent dragging due to the electron–electron interaction, which is given by

$$\alpha_\sigma = 1 - 2 j_1 I_\sigma - 2 j_2 I_{-\sigma}, \tag{3}$$

where I_σ is the bond-charge defined by

$$I_\sigma \equiv \langle c^{\dagger}_{i\sigma} c_{j\sigma} \rangle = -\frac{2}{D} \int_{-\infty}^{\varepsilon_{\text{F}\sigma}} \varepsilon N(\varepsilon)\, \mathrm{d}\varepsilon. \tag{4}$$

Here $N(\varepsilon)$ is the DOS, and $D \equiv 2zt$ is the bare electron bandwidth with z being the number of nearest neighbours. ε^0_{F} and $\varepsilon_{\text{F}\sigma}$ are the Fermi energies for the bare and the renormalized

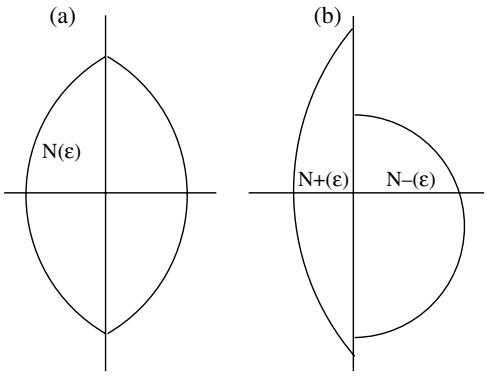

Figure 2. Schematic diagram of the DOS showing the bandwidth change for a magnetic system with finite j_1 and j_2: (a) paramagnetic DOS and (b) ferromagnetic DOS.

electron band, respectively. To simplify the notation, we introduced the following parameters:

$$j_1 = \frac{1}{2}\left(\frac{J_{\rm ex}}{t} - \frac{V}{t}\right), \qquad j_2 = \frac{1}{2}\left(\frac{J_{\rm ex}}{t} + \frac{J_{\rm ph}}{t}\right)$$
$$\tilde{u} = \frac{U}{D} + \frac{zJ_{\rm ex}}{D}. \tag{5}$$

$\tilde{u}$ plays a role of the effective Stoner parameter. As shown in figure 2, the bandwidth will be changed due to the spin-dependent α_σ.

To obtain the equilibrium magnetization m for given interaction parameters at zero temperature, one should find a global minimum of the total energy with respect to m,

$$E = \langle H \rangle = -\frac{D}{2}\sum_\sigma \left(I_\sigma - j_1 I_\sigma^2 - j_2 I_\sigma I_{-\sigma}\right) + \frac{\tilde{u}D}{4}(n^2 - m^2), \tag{6}$$

with the constraint of the particle number conservation,

$$\tfrac{1}{2}m = \int_{\varepsilon_{\rm F}^0}^{\varepsilon_{{\rm F}\sigma}} \sigma N(\varepsilon)\,{\rm d}\varepsilon. \tag{7}$$

Then the equilibrium m can be obtained by minimizing $E(m)$ within the range $0 < m < n$.

Let us first find the local extrema which satisfy

$$\partial_m E = 0. \tag{8}$$

Here ∂_m represents $\frac{\partial}{\partial m}$. Differentiating equation (6) by m, one gets

$$\partial_m E = -\frac{D}{2}\sum_\sigma \{(1 - 2j_1 I_\sigma - 2j_2 I_{-\sigma})\partial_m I_\sigma\} - \frac{\tilde{u}D}{2}m. \tag{9}$$

Differentiation of equation (7) by m gives

$$\tfrac{1}{2} = (\partial_m \varepsilon_{{\rm F}\sigma})\sigma N(\varepsilon_{{\rm F}\sigma}). \tag{10}$$

Using equations (4) and (10), one gets an expression for $\partial_m I_\sigma$:

$$\begin{aligned}\partial_m I_\sigma &= \partial_m \frac{2}{D}\int_{-\infty}^{\varepsilon_{{\rm F}\sigma}} -\varepsilon N(\varepsilon)\,{\rm d}\varepsilon \\ &= -\frac{2}{D}(\partial_m \varepsilon_{{\rm F}\sigma})\varepsilon_{{\rm F}\sigma} N(\varepsilon_{{\rm F}\sigma}) \\ &= -\frac{\sigma \varepsilon_{{\rm F}\sigma}}{D}.\end{aligned} \tag{11}$$

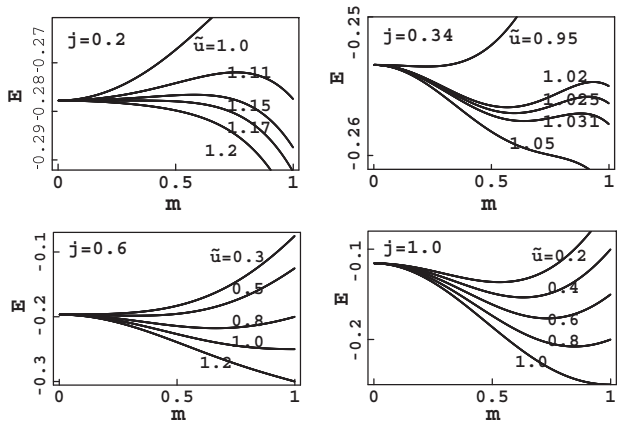

Figure 3. Total energy E as a function of magnetization m for the half-filled 1D TB-DOS ($n = 1$). We vary the $(j, \tilde{u})$ parameters with fixing $\beta = 1$ ($j_1 = j_2 = j$).

Then the local extrema are obtained by the following equation:

$$\begin{aligned} 0 &= \partial_m E \\ &= \frac{1}{2}\sum_{\sigma} \sigma \left(\alpha_\sigma \varepsilon_{\mathrm{F}\sigma} - \frac{\sigma}{2}\tilde{u} D m\right) \\ &\equiv D(\varepsilon_+ - \varepsilon_-). \end{aligned} \tag{12}$$

Note that Hirsch used this condition to obtain the magnetic phase diagram. However, as mentioned earlier, one should get the global minimum of the total energy to determine the equilibrium magnetization. That is, finding just the local extrema from equation (12) and checking the Stoner criterion would not be sufficient. This is because (i) the Stoner criterion is not a sufficient but a necessary condition for the ferromagnetic instability [6], and (ii) there is a constraint for the magnetization: $0 < m < n$. Therefore one should compare the total energy at the extremum m with those at $m = 0$ and $m = n$.

In figure 3, we plot the total energy E as a function of m for the 1D TB-DOS by varying the $(j, \tilde{u})$ parameters. The 1D TB-DOS is given by

$$N(\varepsilon) = \frac{1}{\pi\sqrt{1/4 - \varepsilon^2}} \tag{13}$$

for each spin, and thus the DOS is fully filled for $n = 2$. D is taken to be 1 for calculational simplicity. In figure 3, we have considered the half-filled case ($n = 1$). We have also introduced a parameter β such that $j_2 \equiv j$ and $j_1 \equiv \beta j$, that is, $\beta = (J_{\mathrm{ex}} - V)/(J_{\mathrm{ex}} + J_{\mathrm{ph}})$. Let us first consider the case of $\beta = 1$. The case of $\beta \neq 1$ will be discussed with respect to figure 8. For $j = 0.2$, the Stoner criterion is satisfied when $\tilde{u} \sim 1.25$, implying that the paramagnetic (PM) state becomes unstable for $j = 0.2$ and $\tilde{u} > 1.25$. But, as seen in the figure, the ferromagnetic (FM) state with finite m is already more stable than the PM state even when $\tilde{u} < 1.25$. This indicates that the Stoner criterion is only a necessary condition for the ferromagnetism. Also noteworthy is that the condition $\partial_m E|_{m=1} < 0$ will not give the criterion of a global minimum but only a local minimum for the fully polarized ferromagnetic (FFM) state ($m = n$). For $j = 0.34$, as $\tilde{u}$ increases, the magnetization increases continuously from $m = 0$ to $m \sim 0.6$, and at $\tilde{u} \sim 1.025$, it jumps from $m \sim 0.6$ to $m = 1$ discontinuously. For $j = 0.6$, the magnetization increases from $m = 0$ to 1 continuously as $\tilde{u}$ increases up to 1. For $j = 1.0$, the magnetization increases continuously from $m \sim 0.4$ to $m = 1$. The case of $j = 0.34$

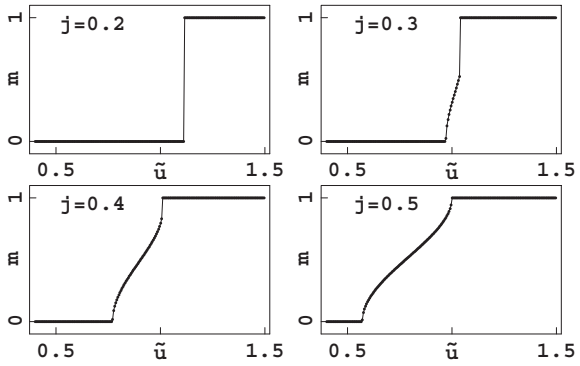

Figure 4. Magnetization as a function of $\tilde{u}$ for the half-filled 1D TB-DOS with $\beta = 1$. For small values of j, the magnetization jumps discontinuously from 0 to 1. For larger value of j, the magnetization increases smoothly, so the partially magnetized region appears.

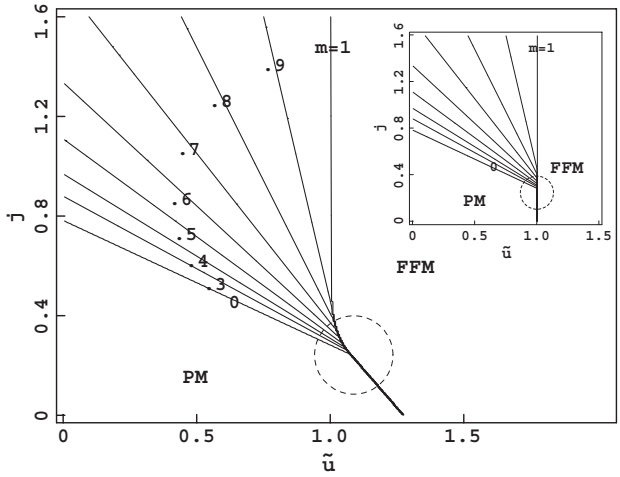

Figure 5. Magnetic phase diagram for the half-filled 1D TB-DOS in the (j–$\tilde{u}$) space with $\beta = 1$. FFM represents the fully polarized ferromagnetic phase, and PM represents the paramagnetic phase. The region between them corresponds to the partially polarized ferromagnetic (PFM) phase with finite magnetization. The inset shows the phase diagram obtained by Hirsch [3] employing the local minimum search. The lines in the PFM region correspond to extrema lines for given magnetization values. Note the difference between the present and Hirsch's results near the vertex region (circled area).

demonstrates the necessity of using the total energy minimization to obtain the correct magnetic phase.

Figure 4 presents the magnetization as a function of $\tilde{u}$ for the half-filled 1D TB-DOS with $\beta = 1$. For $j = 0.2$, as $\tilde{u}$ increases, the system transforms from the PM phase to the FFM phase directly. On the other hand, for $j = 0.3$ and 0.4, as $\tilde{u}$ increases, the magnetization goes from 0 to finite value smoothly, and at some $\tilde{u}$, it jumps to 1. For $j = 0.5$, the magnetization increases from 0 to 1 smoothly. For much larger value of j, say $j = 1.0$, the magnetization starts from a finite value and increases smoothly to 1.

In figure 5, we present the resulting magnetic phase diagram for the 1D TB-DOS with varying j and $\tilde{u}$ parameters. The magnetization here is obtained by the total energy

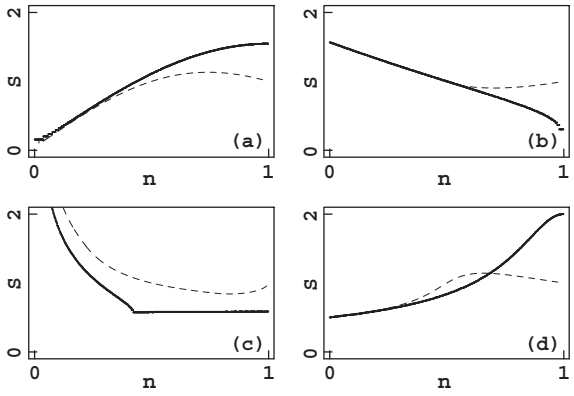

Figure 6. $S(n,m) \equiv (\varepsilon_{F\uparrow} - \varepsilon_{F\downarrow})/m$ as a function of n for the (a) 1D, (b) 2D, (c) 3D TB-DOSs, and (d) the parabolic DOS. Solid lines correspond to $m = 0$ and dotted lines to $m = n$.

minimization. For small j and $\tilde{u}$, the PM phase is stable, while for large j and $\tilde{u}$, the FFM phase is stable. The partially polarized FM phase (PFM) is stable in between. The result is nearly the same as that of Hirsch [3] (see the inset of figure 5). But there is also a noticeable difference near $\tilde{u} \sim 1$ for small j near the vertex region. According to the result by Hirsch, the FFM phase is always stable for $\tilde{u} > 1$. In contrast, in the correct magnetic phase diagram, there are regions of stable PFM and PM phases even for $\tilde{u} > 1$. In fact, the PFM region appears only for $\tilde{u} < 1/(\pi/2 - 2/\pi) \approx 1.07$, at which the boundary line between the PM and FFM phases for small j and the extremum line for $m = 0$ intersect.

Let us check more carefully when the local minima search and the total energy minimization yield different results. If there is more than one extremum between $m = 0$ and 1, as we have seen for $j = 0.34$ in figure 3, the local minima search and the total energy minimization can give different results. To have more than one extremum, extrema lines for certain magnetization values in the (j–$\tilde{u}$) space must intersect. From equation (12), one gets the extremum line for given magnetization,

$$\begin{aligned} j &= \frac{(\varepsilon_{F\uparrow} - \varepsilon_{F\downarrow}) - \tilde{u}m}{2\beta(I_\uparrow \varepsilon_{F\uparrow} - I_\downarrow \varepsilon_{F\downarrow}) + 2(I_\downarrow \varepsilon_{F\uparrow} I_\uparrow \varepsilon_{F\downarrow})} \\ &= \frac{(\varepsilon_{F\uparrow} - \varepsilon_{F\downarrow})\left(1 - \tilde{u}\frac{m}{(\varepsilon_{F\uparrow} - \varepsilon_{F\downarrow})}\right)}{2\beta(I_\uparrow \varepsilon_{F\uparrow} - I_\downarrow \varepsilon_{F\downarrow}) + 2(I_\downarrow \varepsilon_{F\uparrow} I_\uparrow \varepsilon_{F\downarrow})} \\ &\equiv j_0(n,m)\left(1 - \frac{\tilde{u}}{(\varepsilon_{F\uparrow} - \varepsilon_{F\downarrow})/m}\right) \\ &\equiv j_0(n,m)\left(1 - \frac{\tilde{u}}{S(n,m)}\right). \end{aligned} \tag{14}$$

Equation (14) indicates that the intersections of the extremum line with j and $\tilde{u}$ axes are $j_0(n,m)$ and $S(n,m)$, respectively. Here $j_0(n,m)$ corresponds to the j-value that gives the extremum energy at m for given n and $\tilde{u} = 0$, while $S(n,m) \equiv (\varepsilon_{F\uparrow} - \varepsilon_{F\downarrow})/m$ corresponds to the $\tilde{u}$-value that gives the extremum energy at m for given n and $j = 0$.

In figure 6, we show $S(n,0)$ and $S(n,n)$ as a function of n for several DOSs. The boundary between the PM and FM phases is determined by the value of $S(n,0)$ which corresponds to $\partial_m(\varepsilon_{F\uparrow} - \varepsilon_{F\downarrow})|_{m=0}$, whereas the boundary between the PFM and FFM phases is determined by the value of $S(n,n)$. Note that for the 2D (figure 6(b)) and 3D (figure 6(c)) TB-DOSs,

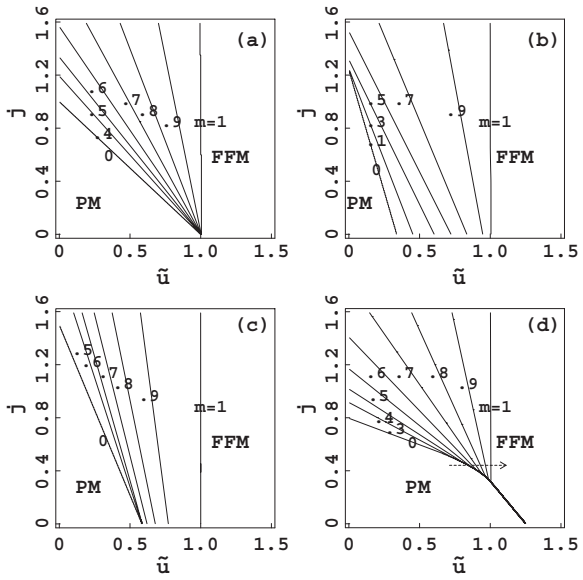

Figure 7. Magnetic phase diagram for the square-type DOS (a), the 2D (b) and 3D (c) TB-DOSs, and the parabolic DOS (d) in the $(j–\tilde{u})$ space. We consider the case with $\beta = 1$ and $n = 1$ (half-filled case). Only for the parabolic DOS does the PM–FFM boundary appear.

$S(n, n)$ is always larger than $S(n, 0)$, while for the 1D TB-DOS (figure 6(a)) and the parabolic DOS (figure 6(d)), they are reversed for some region of n. The square-type DOS is special, because $S(n, m)$ is always one for any m. To be precise, one should check whether $S(n, m)$ is a monotonically increasing function of m or not. Note that, for $\beta > 0$, $j_0(n, m)$ is a monotonically increasing function of m. Therefore, provided

$$S(n, m_1) < S(n, m_2), \tag{15}$$

for $m_1 > m_2$, there are always intersections between extrema lines of m_1 and m_2, and so there is eventually more than one extremum in some region. Thus, one can conclude from the results of figure 6 that, for the 1D TB-DOS and the parabolic DOS, the local minima search and the total energy minimization yield different results, while, for the 2D and 3D TB-DOSs and the square-type DOS, both methods yield the same results[1].

One can generalize this argument to the cases with the arbitrary DOS form. That is, if the DOS shape is of a concave type (high at the band edge and low at the band centre) as for the 1D TB-DOS, the inequality of equation (15) holds and so the local minima search and the total energy minimization will produce different results. Then there may be some jumps in the magnetization, as seen in figure 4.

In figure 7, we have plotted the magnetic phase diagram in the $(j–\tilde{u})$ space for the half-filled case and $\beta = 1$. It is seen that both j and $\tilde{u}$ enhance the ferromagnetism. As expected, only for the parabolic DOS (figure 7(d)), which is of a concave type, does a direct boundary between the PM and FFM phases appear. The comparison between figures 5 and 7(d) clearly shows a modification of the magnetic phase diagram due to the change in the DOS shape. As $\tilde{u}$ increases along the horizontal arrow in figure 7(d), the magnetization jumps first from 0 to a

[1] This is valid for $\beta > 0$. For $\beta < 0$, caution is needed, because $j_0(n, m)$ is not always a monotonically increasing function of m (see [5]).

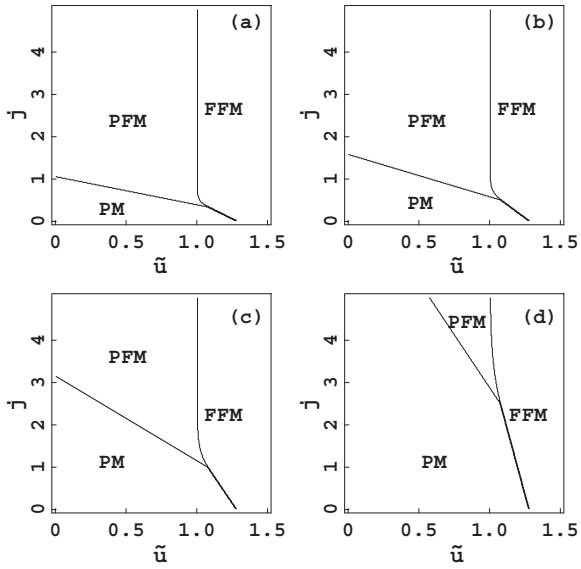

Figure 8. Magnetic phase diagram for the half-filled 1D TB-DOS in the (j–$\tilde{u}$) space with varying the β parameter. (a) $\beta = 0.5$, (b) $\beta = 0$, (c) $\beta = -0.5$, (d) $\beta = -0.8$. As β decreases, the PFM region becomes narrower.

finite value and then grows continuously to 1. This behaviour is different from that for the 1D TB-DOS (figure 5).

In figure 8, we have provided the magnetic phase diagram in the (j–$\tilde{u}$) space, for the 1D TB-DOS with varying β-value. As β decreases, the PFM region becomes narrower, and so for $\beta < -1$, the PFM region disappears completely. Note that varying β corresponds to changing the ratio of $(J_{ex} - V)/(J_{ex} + J_{ph})$, that is, incorporating the inter-site Coulomb interaction and the pair-hopping interaction effectively in the exchange interaction. The results of figure 8 reflect that the effects of the inter-site Coulomb and the pair-hopping interaction on the ferromagnetism would be important for some cases. This behaviour is for the half-filled case. For different band fillings, the β-dependence is a bit different [7].

In figure 9, we plot the bandwidth parameter α_σ as a function of $\tilde{u}$ for the 1D TB-DOS, with varying other parameters (β, j, and n). In the case of figure 9(a), as $\tilde{u}$ increases, the α_σ for both spins increase equally. Since α_σ is a function of m for given j, n, and β, one can deduce from figure 9(a) that, as $\tilde{u}$ increases, the magnetic phase changes from the PM to the PFM phase, and then to the FFM phase. The situation in figure 9(b) is similar to that in figure 9(a) except that the bandwidth parameter is different for each spin. The bandwidth of the minority spin is narrower than that of the majority spin. We have from equation (3) that

$$\alpha_\uparrow - \alpha_\downarrow = 2j(I_\uparrow - I_\downarrow)(1 - \beta). \tag{16}$$

$I_\sigma(n)$ has a dome-like shape with maximum at $n = 1$, and so $I_\uparrow > I_\downarrow$ below half-filling. Accordingly, $\alpha_\uparrow \geqslant \alpha_\downarrow$ for $\beta \leqslant 1$, as shown in figure 9. For $\beta = 1$, α_σ for both spins are equal, as mentioned in figure 9(a). In the case of a half-filled symmetric band, the α_σ for both spins are equal too.

In figure 10, we present the magnetic phase diagram in the (n–j) space for the 1D TB-DOS, with varying β. We fixed $\tilde{u} = 0.2$. As β decreases, the PFM region becomes narrower, while the PM region becomes wider near the half-filling. The FFM phase becomes the most

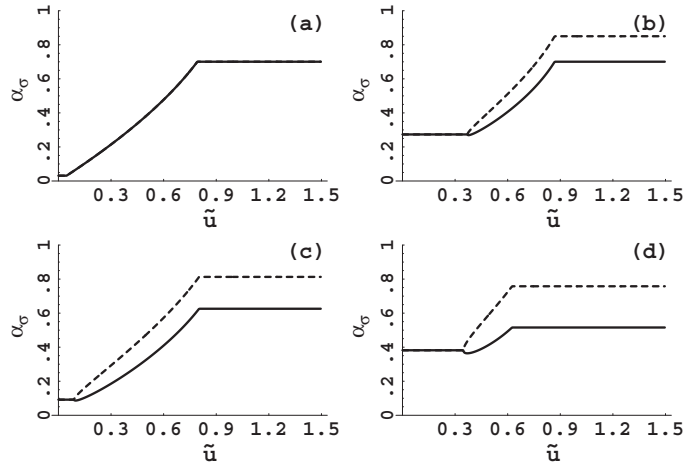

Figure 9. Bandwidth parameter α_σ as a function of $\tilde{u}$ for the 1D TB-DOS with varying (a, j, n) parameters. (a) $\beta = 1$, $j = 0.8$, $n = 0.8$, (b) $\beta = 0.5$, $j = 0.8$, $n = 0.8$, (c) $\beta = 0.5$, $j = 1.0$, $n = 0.8$, and (d) $\beta = 0.5$, $j = 0.8$, $n = 0.6$. The dotted line is for the majority spin and the solid one is for the minority spin.

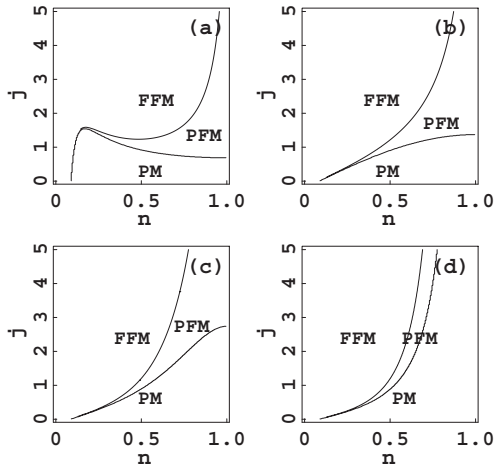

Figure 10. Magnetic phase diagram for the 1D TB-DOS in the $(n–j)$ space with varying β. We fixed $\tilde{u} = 0.2$. (a) $\beta = 1$, (b) $\beta = 0$, (c) $\beta = -0.5$, and (d) $\beta = -1$.

stable near the band edge. Note that $\alpha_\sigma = 1 - 2j(I_{-\sigma} - I_\sigma)$ for $\beta = -1$, and so the effect of the bandwidth change becomes negligible near half-filling where $I_\uparrow \approx I_\downarrow$.

We have also checked the β-dependence of the magnetic phase diagram for other DOSs, and found that the β-dependence is similar to that for 1D TB-DOS. From figures 7 and 10, one can argue that both j and $\tilde{u}$ enhance the ferromagnetism, while V enhances the ferromagnetism near band edges. On the other hand, $J_{\rm ph}$ enhances the ferromagnetism, but the enhanced region relies on the sign of $J_{\rm ex} - V$. That is, for positive $J_{\rm ex} - V$, the ferromagnetism near the band centre is enhanced, whereas, for negative $J_{\rm ex} - V$, the ferromagnetism near band edges is enhanced.

In conclusion, we have obtained the magnetic phase diagrams for several DOS shapes by varying the electron–electron interaction parameters. We have demonstrated that the DOS shape significantly affects the properties near the magnetic phase boundaries. We have verified that the total energy minimization is essential for obtaining the correct magnetic phase diagram. We have also found the relationship between the DOS shape and the magnetization behaviour, which reveals that a system with the DOS shape of a concave type could have a discontinuous magnetization jump as the effective Stoner parameter $\tilde{u}$ increases.

Acknowledgments

This work was supported by the SRC/ERC program of MOST/KOSEF (R11-2000-071) and by the Basic Research Program of the KOSEF (R01-2006-000-10369-0).

References

[1] Hirsch J E 1999 *Phys. Rev.* B **59** 436
[2] Hirsch J E 1999 *Phys. Rev.* B **59** 6256
[3] Hirsch J E 1990 *Phys. Rev.* B **42** 771
[4] Hirsch J E 1991 *Phys. Rev.* B **44** 675
[5] Barreteau C, Desjonqueres M-C, Oles A M and Spanjaard D 2004 *Phys. Rev.* B **69** 064432
[6] Wohlfarth E P 1976 *Magnetism* ed S Foner (London: Gordon and Breach Science) chapter 2
[7] Kim K 2006 unpublished